Design of Drilled Shafts Supporting Highway Signs

John L. Davidson and Clifford O. Hays, Jr., Department of Civil Engineering, University of Florida, Gainesville
Eugene M. Hagan, Jr.,* Harbor Engineering Company, Jacksonville, Florida

The general behavior of single drilled shafts subjected to lateral loads and of their design methods are reviewed. Such shafts can economically be used as sign supports in highway work. A simplified but accurate design method that assumes rigid-body motion of the pile and that the lateral soil resistance varies linearly with the depth at ultimate load but reverses direction at the point of rotation of the shaft is developed. Charts are given for routine design. Methods for determining the maximum soil resistance at the surface and the slope of its assumed linear variation are reviewed and conservative recommendations are made for determining these values. Methods for determining the soil-strength parameters for the analysis are reviewed and design examples are given for both cohesive and cohesionless soils.

The foundations that support the large overhead signs on modern multilane highways typically consist of shallow, reinforced-concrete spread footings. A possible economical alternative to these large footings, which would resist the high wind-induced moments, is a drilled-shaft foundation, constructed by augering a hole, inserting a prefabricated reinforcing cage, and filling it with concrete.

This paper briefly examines the analysis and behavior of drilled shafts and presents a simplified design method (in chart form) for short pile foundations subject to lateral loading. The proposed procedure considers two fundamental facts about pile behavior that are often overlooked in approximate design methods: (a) The lateral force distribution in the soil along the pile is a function of the deflected shape of the pile even if limiting values of soil resistance are developed and (b) the limiting values of the lateral soil force will generally increase with depth within any soil layer.

The behavior of a pile depends on its length. In long piles, failure occurs when a plastic hinge forms at the point of maximum bending moment. Thus, pile deflections are very important since they affect the soil pressure and the bending moment, particularly if there are significant axial loads. In short piles having lengths less than about 10 times their diameter, failure occurs when the lateral soil resistance is exceeded and rigid-body rotation occurs. Drilled-shaft foundations of the size used for typical highway sign loads are normally designed as rigid short piles.

PREVIOUS WORK

Seiler (17) assumed a parabolic soil-resistance distribution and developed design charts for the depth of embedment of timber poles. This pressure distribution, which was confirmed by Rutledge (15), Osterberg (14), and Shilts and others (18), satisfies statics and qualitatively recognizes the force-deformation response of the soil, but makes several arbitrary assumptions including the location of the point of zero soil resistance. Rutledge (15) has developed a nomographic embedment chart that assumes the point of rotation of the pole to be at a depth of $\frac{2}{3}$ the embedment and the distribution of soil resistance to be parabolic.

Hansen (5) has developed a method for computing the ultimate load on rigid piles that recognizes the influence of the deflected shape on the lateral soil-resistance distribution. This method most closely resembles the rigid-body design method presented here.

Matlock (12) recommends a Winkler analysis in which the soil is considered to be a series of independent layers that provide a resistance (p) to the pile deflection (y) and has developed criteria (13) for predicting the nonlinear p versus y curves for soft clays, while Parker and Reese (16) have developed criteria for sand, and Welch (20) for stiff clay.

Ivey and others (9, 10, 11) have developed a theory for determining the ultimate resistance of drilled-shaft footings subject to overturning loads. By including all of the shear stresses acting on the pile, a three-dimensional ultimate load solution to the drilled-shaft problem is obtained. Ivey, Koch, and Raba (10) have conducted model pile tests in both sand and clay.

Broms (1, 2, 3), in a series of three articles, discusses the lateral resistance and design of piles in cohesive and cohesionless soils.

A rigorous analysis for deformable piles using a com-

Publication of this paper sponsored by Committee on Foundations of Bridges and Other Structures.

*Mr. Hagan was at the University of Florida when this research was performed.

puter program designated FRAME 51 has been developed by Hays and Matlock (7). This program performs a nonlinear, discrete-element analysis and can be used to obtain the complete load-deformation response of a pile in a layered soil until failure occurs. The program was verified by using actual test results from laterally and axially loaded piles and frames supported on piles (6).

Figure 1. Ultimate soil resistance for cohesive soil.

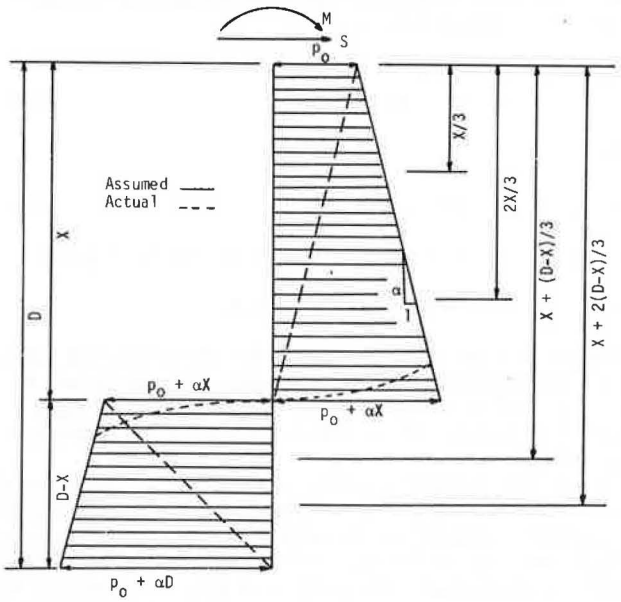

Figure 2. Design chart for cohesive soils.

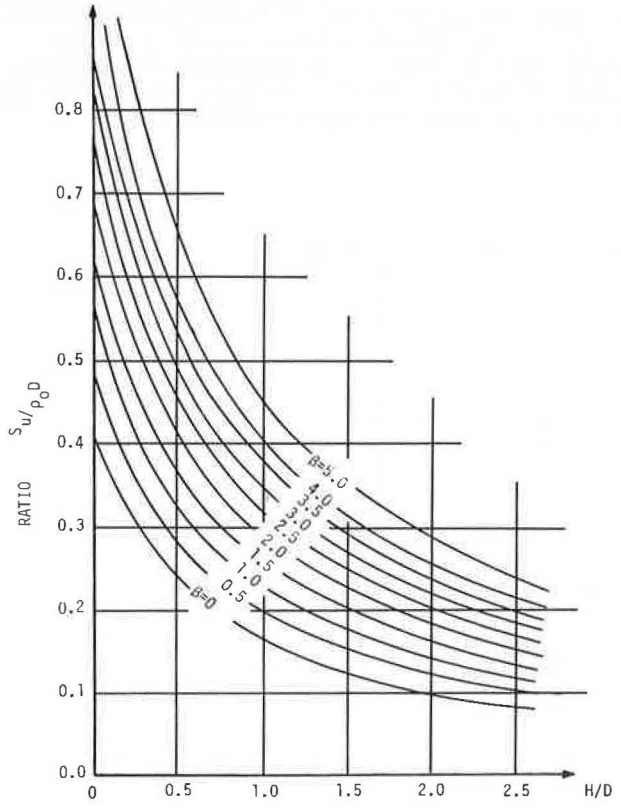

LOAD-DEFLECTION SOLUTION FOR RIGID PILE

Two methods for solution of a rigid-pile model were developed during this research. The first, the more analytical load-deflection procedure, is similar to FRAME 51, but is simpler since only rigid-body motion is involved and the rotation of the pile and the displacement of the ground line define the position of the pile. The nonlinear response of the soil is approximated by discrete nonlinear Winkler springs. Since this model has only two degrees of freedom, a solution procedure could be written for a programmable calculator to handle from one to three soil layers (8).

In the solution of this problem, it was observed that the point of rotation was not at some constant depth, but shifted from somewhere below the middle of the pile-embedment distance for light loads to beyond the three-quarters point for failure loads. The point of rotation varied at ultimate loads for different soils and for different ratios of applied moment to shear. Thus methods that assume a constant location for this point are not truly rational.

ULTIMATE-LOAD SOLUTION FOR RIGID PILE

The solution of the load-deflection program showed that, as the applied load increased to its ultimate value, the soil resistance along the pile increased to its ultimate value along almost the entire length of the pile. (This assumed that premature material failure did not occur and that the p versus y curves had almost unlimited ductility and did not decrease sharply.) This behavior gave rise to the second method of solution of the rigid-pile model, the ultimate-load solution.

Figure 1 shows the actual and assumed soil-resistance distributions at failure for a cohesive soil. By applying statics to this ultimate soil resistance, we can find values of the applied lateral load (S) and the bending moment (M) in terms of the soil parameters, the pile-embedment depth (D), and the unknown distance (X) to the point of rotation. For cohesive soils these are

$$S = p_o(2X - D) + (\alpha/2)(2X^2 - D^2) \quad (1)$$

and

$$M = -p_o(X^2 - D^2/2) - (\alpha/3)(2X^3 - D^3) \quad (2)$$

where

α = slope of the soil resistance diagram, and
p_o = ultimate soil resistance at the ground surface.

If the ratio of X to D is defined as K, and a nondimensional variable (β) defined as

$$\beta = \alpha D/p_o \quad (3)$$

is introduced, then equations 1 and 2 are modified to the nondimensional form

$$S/p_oD = 2K - 1 + \beta(K^2 - 1/2) \quad (4)$$

and

$$(S/p_oD)(H/D) = -K^2 + 1/2 - (\beta/3)(2K^3 - 1) \quad (5)$$

where H is the height above the ground surface to the point where the lateral load is applied. This gives two equations with two unknowns, K and β. A graph was developed for different values of β (Figure 2) to relate

S/p_oD and H/D. The procedure is iterative, with the designer picking a trial embedment depth and then checking the solution to see whether it has adequate strength and converges quickly. Examples for both cohesive and cohesionless soils are given.

Figure 3 shows the actual and assumed soil-resistance distributions at failure for cohesionless soils. By applying statics to the assumed soil distribution, we can find the following equations for S and M.

$$S = (\alpha/2)(2X^2 - D^2) \quad (6)$$

and

$$M = (-\alpha/3)(2X^3 - D^3) \quad (7)$$

Again, if K is defined as the ratio of X to D, the equations are modified to a nondimensional form:

Figure 3. Ultimate soil resistance for cohesionless soil.

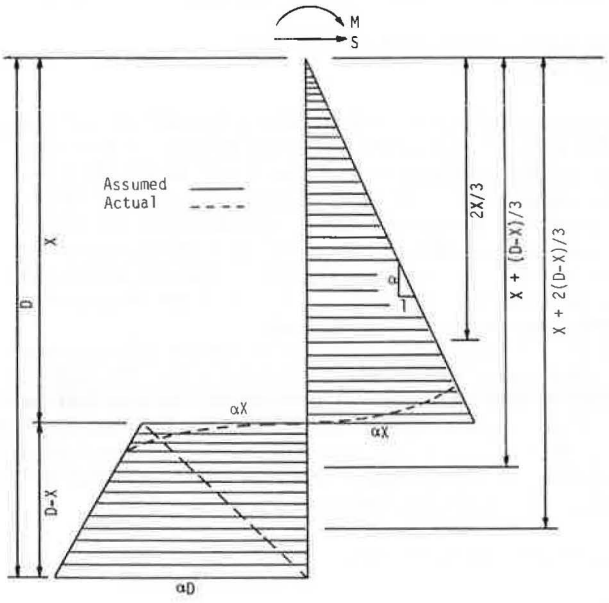

$$S/\alpha D^2 = K^2 - 1/2 \quad (8)$$

and

$$(S/\alpha D^2)(H/D) = (-2/3)K^3 + 1/3 \quad (9)$$

Here again the solution is iterative from the chart in Figure 4.

MAXIMUM MOMENT

The maximum moment (M_{max}) in the pile is not the applied moment, but occurs at a depth (z) below the ground surface. The nondimensional equation for M_{max} in both cohesive and cohesionless soils is

$$M_{max}/M = 1 + z/H - (p_o/\alpha H)\,[(\alpha H^2)(z/H)^2/2S] - (1/3)[(\alpha H^2)(z/H)^3/2S] \quad (10)$$

Thus

$$z/H = [(p_o/\alpha H)^2 + 2S/\alpha H^2]^{1/2} - p_o/\alpha H \quad (11)$$

Figure 5 presents a graph for various values of $p_o/\alpha H$.

RECOMMENDED SOIL RESISTANCE

Comparisons of existing theories for predicting the maximum soil resistance with the model tests performed at Texas A&M University gave the resistance value equations given below. These almost always gave conservative results.

A capacity reduction factor (η) similar to the one used in ultimate-strength concrete design is included in these equations to account for the accuracy with which pertinent soil properties are known. This factor should vary from a value close to one when good soils data are available to lower values if only general soils conditions at the site are known.

For cohesionless soils, Broms' assumption (1, 2, 3) of a zero resistance at the ground surface that increases to three times the passive pressure times the pile diameter always gave conservative results. However, in this analysis the soil resistance is assumed to change directions at the point of rotation of the pile. The equation for the slope of the soil-resistance distribution (α) is

Figure 4. Design chart for cohesionless soils.

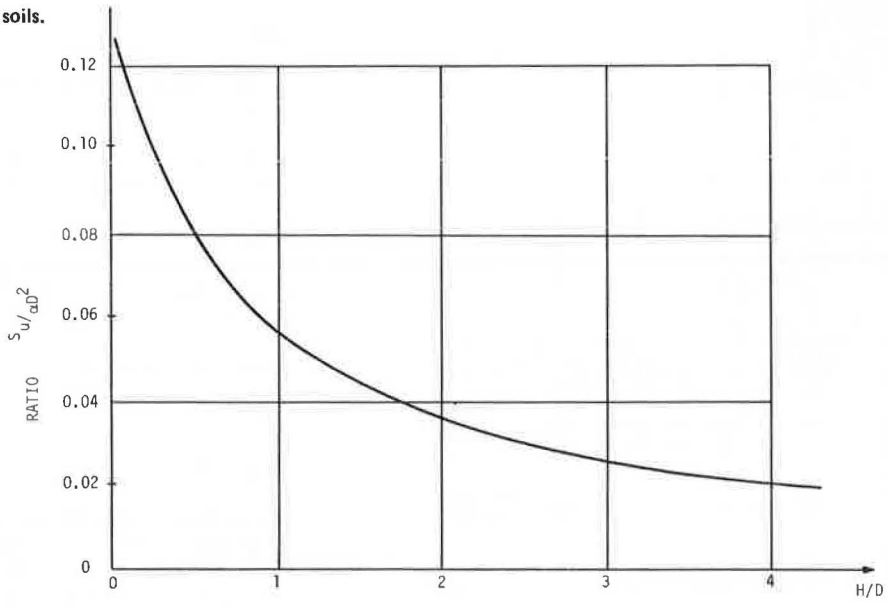

$$\alpha = 3\gamma B \tan^2(45° + \phi/2)\eta \quad (12)$$

where

B = pile diameter,
γ = effective soil unit weight, and
ϕ = angle of internal friction.

For cohesive soils, the criteria developed by Matlock (13) were slightly modified in the direction of conservatism. It was assumed that the ultimate soil resistance begins at the ground level with a value of twice the cohesive strength (c) times the pile diameter (Matlock assumes a factor of three). Thus,

$$p_0 = 2cB\eta \quad (13)$$

The strength then increases to nine times the cohesive strength times the pile diameter at a depth (x_r) below the ground surface, where

$$x_r = 7cB/(\gamma B + 0.5c) \quad (14)$$

To satisfy the assumption of a linear increase in soil resistance, α is determined in one of two ways for cohesive soils. If the required embedment depth is less than x_r, then

$$\alpha = \eta 7cB/X_r \quad (15)$$

This is the actual slope of the soil resistance. If the required embedment depth is greater than x_r, then conservatively

$$\alpha = (7cB/D)\eta \quad (16)$$

Figure 5. Maximum moment chart.

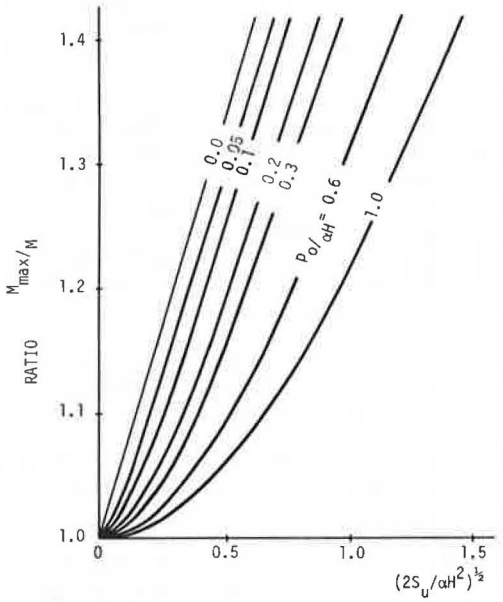

DETERMINATION OF SOIL STRENGTH PARAMETERS

Three different possible procedures exist for determining the soil strength parameters to be used in the design of drilled shafts: laboratory testing of soil samples, in situ field testing, and estimation of the properties by a visual inspection of the soil.

The most frequently used laboratory test on undisturbed clay samples is the unconfined compression test, but triaxial UU and CU tests, miniature vane shear, and pocket penetrometer tests can also be used. For cohesionless soils, the angle of internal friction (ϕ) may be determined in the laboratory by direct shear testing.

There are several field tests that provide values of c and ϕ or both for in situ soil. These include standard penetration, static cone penetration, pressuremeter, and Iowa bore-hole shear testing.

If no soil testing is done or if preliminary numbers are desired, estimates of values of c and ϕ can be made by inspection. For cohesionless soil, the ease with which

Table 1. Comparison of analyses with results of Texas A&M tests.

Test Number	Type of Soil[a]	H (m)	D (m)	H/D	B (m)	p_0 (N/m²)	α (N/m³)	β	Ultimate Load (N) Actual	Solution Theory	A&M Theory	Solution Theory/ Actual	A&M Theory/ Actual
5-1	1	0.610	0.305	2	0.102	0	1951	–	1356	752	1557	0.555	1.15
5-2	1	0.610	0.305	2	0.102	0	1951	–	1629	752	1557	0.462	0.956
5-3	1	0.610	0.305	2	0.102	0	1951	–	1346	752	1557	0.559	1.16
5-4	1	0.610	0.305	2	0.102	0	1951	–	1423	752	1557	0.529	1.09
5-5	1	0.509	0.254	2	0.102	0	1951	–	958	524	1145	0.546	1.20
5-6	1	0.610	0.305	2	0.102	0	1951	–	1581	752	1557	0.476	0.985
5-7	1	0.610	0.305	2	0.102	0	1951	–	1250	752	1557	0.602	1.25
5-8	1	0.509	0.254	2	0.102	0	1951	–	1054	524	1145	0.497	1.09
5-9	1	0.558	0.254	2	0.102	0	1951	–	886	524	1145	0.591	1.29
5-10	1	0.254	0.254	1	0.102	0	1951	–	1605	820	1830	0.512	1.14
5-11	1	0.610	0.305	2	0.076	0	1464	–	1054	566	1116	0.537	1.06
5-12	1	0.305	0.305	1	0.076	0	1464	–	2299	884	2433	0.384	1.06
5-13	1	0.610	0.305	2	0.051	0	975	–	1068	377	714	0.353	0.668
5-14	1	0.305	0.305	1	0.102	0	1951	–	2491	1178	2515	0.473	1.01
5-15	1	0	0.305	0	0.102	0	1951	–	5509	2730	6419	0.496	1.17
5-16	2	0.610	0.305	2	0.102	0	1477	–	445	571	1087	1.28	2.44
5-17	2	0.610	0.305	2	0.102	0	1477	–	685	571	1087	0.833	1.59
E-1	3	0.509	0.254	2	0.102	8335	7525	0.75	23854	11515	21986	0.483	0.922
E-2	3	1.069	0.305	3.5	0.102	8335	7525	0.903	19639	8526	16142	0.434	0.822
E-3	3	0.610	0.305	2	0.102	8335	7525	0.903	23950	11889	25627	0.496	1.07
E-4	3	0.305	0.305	1	0.102	8335	7525	0.903	29459	19735	41721	0.670	1.42
E-5	3	0.610	0.305	2	0.076	6252	7467	1.19	16861	9757	18394	0.579	1.09
C-1	4	0.509	0.254	2	0.102	11245	10057	0.745	11783	12909	14370	1.10	1.22
C-2	4	0.610	0.305	2	0.102	11245	10057	0.894	17100	15855	16478	0.927	0.964
C-3	4	0.610	0.305	2	0.076	8433	10004	1.19	13891	13072	11544	0.941	0.831

Notes: 1 m = 3.28 ft; 1 N = 0.021 lbf; 1 N/m² = 0.225 lb/ft²; 1 N/m³ = 0.735 lb/ft³; η = 1.

[a]For soil 1, c = 0, ϕ = 37°, and γ = 148 N/m³; for soil 2, c = 0, ϕ = 32°, and γ = 139 N/m³; for soil 3, c = 12 505 N/m², ϕ = 9°, and γ = 181 N/m³; and for soil 4, c = 16 866 N/m², ϕ = 0°, and γ = 171 N/m³.

a 0.5-in diameter reinforcing bar can be pushed into the soil has been related to the relative density [Cooling, Skempton, and Glossup (4)], which can then be related to ϕ [Terzaghi and Peck (19)]. For clays, the ease with which a specimen of the soil can be deformed between the fingers has been related to stiffness [Cooling, Skempton, and Glossup (4)], which can be related to the undrained strength [Terzaghi and Peck (19)].

The soil strength reduction factor has been used in the equations to account for the possibility of the soil having less than the anticipated strength and for any discrepancies in the simplified theory. The choice of this factor should reflect how well the actual soil strength is known. The following values are recommended:

η	Quality of Soil Information
0.5	Good visual description possibly supplemented by standard penetration testing in general area
0.7	Standard penetration testing or other in situ testing at location of structure
0.9	Laboratory testing at location of structure

Since a drilled shaft is essentially a deep foundation, the soil at the bottom of the shaft is as important as that near the surface (8), and whenever only limited soil tests have been performed, a close inspection procedure during construction should be followed so that, if weak soil layers are encountered, the shaft length can be increased.

TEXAS A&M MODEL TESTS

Ivey (10, 11) has conducted a number of model and full-scale drilled-shaft tests. Details of the model tests are given in Table 1 with the Texas A&M predictions, and predictions made using the ultimate-load solution described here. The Texas A&M theory usually gave unconservative answers; the mean prediction was 1.15 times that of the actual observed ultimate loads. The ultimate-load solution was almost always conservative; the mean was 0.61 times that of the observed mean. A reason for this conservatism is the relatively low D/B ratios of the models that imply that there will be some footing action that was neglected in the analysis. Load-deflection solutions (8) using the rigid discrete-pile model confirmed that the ultimate-load solution was adequate, provided that the pile was designed to have sufficient strength. In fact, solutions with the discrete model (8) showed that, even for long piles, the ultimate-load solution is adequate provided that there are no significant axial loads and that the magnitude of deflections is not important. Most highway sign structures would satisfy these criteria.

REFERENCES

1. B. B. Broms. Lateral Resistance of Piles in Cohesive Soils. Journal of the Soil Mechanics and Foundations Division, Proc., ASCE, Vol. 90, No. SM2, March 1964, pp. 27-63.
2. B. B. Broms. Lateral Resistance of Piles in Cohesionless Soils. Journal of the Soil Mechanics and Foundations Division, Proc., ASCE, Vol. 90, No. SM3, May 1964, pp. 123-156.
3. B. B. Broms. Design of Laterally Loaded Piles. Journal of the Soil Mechanics and Foundations Division, Proc., ASCE, Vol. 91, No. SM3, May 1965, pp. 79-99.
4. L. F. Cooling, A. W. Skempton, and R. Glossup. Discussion of Classification and Identification of Soils by A. Casagrande. Trans., ASCE, Vol. 133, 1948, p. 966.
5. J. B. Hansen. The Ultimate Resistance of Rigid Piles Against Transversal Lateral Forces. Danish Geotechnical Institute, Bulletin 12, 1961.
6. C. O. Hays and H. Matlock. A Nonlinear Analysis of Statically Loaded Plane Frames Using a Discrete Element Model. Center for Highway Research, Univ. of Texas at Austin, Research Rept. 56-23, May 1972.
7. C. O. Hays, Jr., and H. Matlock. Nonlinear Discrete Element Analysis of Frames. Journal of Structural Division, Proc., ASCE, Vol. 99, No. ST10, Oct. 1973, pp. 2011-2030.
8. C. O. Hays, Jr., J. L. Davidson, E. M. Hagan, and R. R. Risitano. Drilled Shaft Foundation for Highway Sign Structures. Engineering and Industrial Experiment Station, Univ. of Florida, Gainesville, Research Rept. D647F, Dec. 1974.
9. D. L. Ivey. Theory, Resistance of a Drilled Shaft Footing to Overturning Loads, Model Tests and Correlation With Theory. Texas Transportation Institute, Texas A&M Univ., College Station, Research Rept. 105-1, Feb. 1968.
10. D. L. Ivey, K. J. Koch, and C. F. Raba, Jr. Resistance of a Drilled Shaft Footing to Overturning Loads, Model Tests and Correlation With Theory. Texas Transportation Institute, Texas A&M Univ., College Station, Research Rept. 105-2, July 1968.
11. D. L. Ivey and W. A. Dunlap. Design Procedure Compared to Full-Scale Tests of Drilled Shaft Footings. Texas Transportation Institute, Texas A&M Univ., College Station, Research Rept. 105-3, Feb. 1970.
12. H. Matlock. Correlations for Design of Laterally Loaded Piles in Soft Clay. 2nd Annual Offshore Technology Conference, Houston, Texas, Paper OTX 1204, Feb. 1970.
13. H. Matlock and L. C. Reese. Generalized Solutions for Laterally Loaded Piles. Journal of the Soil Mechanics Division, Proc., ASCE, Vol. 86, No. SM5, Oct. 1961, pp. 673-694.
14. J. O. Osterberg. Lateral Stability of Poles Embedded in Clay Soil. Northwestern Univ. Project 208; Bell Telephone Laboratories, Evanston, Ill., Dec. 1958.
15. Engineering Manual. Outdoor Advertising Association of America, Chicago, 1955.
16. F. Parker, Jr., and L. C. Reese. Experimental and Analytical Studies of Behavior of Single Piles in Sand Under Lateral and Axial Loading. Center for Highway Research, Univ. of Texas at Austin, Research Rept. 117-2, 1971.
17. J. F. Seiler. Effect of Depth of Embedment on Pole Stability. Wood Preserving News, Vol. 10, No. 11, Nov. 1932, pp. 152-161.
18. W. L. Shilts, L. D. Gaves, and G. G. Driscoll. A Report of Field and Laboratory Tests on the Stability of Posts Against Lateral Loads. Proc., 2nd International Conference on Soil Mechanics and Foundation Engineering, Vol. 5, Rotterdam, Holland, 1948, pp. 107-122.
19. K. Terzaghi and R. B. Peck. Soil Mechanics in Engineering Practice, 2nd Ed. Wiley, New York, 1967.
20. R. C. Welch and L. C. Reese. Lateral Load Behavior of Drilled Shafts. Center for Highway Research, Univ. of Texas at Austin, Research Rept. 89-10, May 1972, pp. 99-106.